

A new approach to the dynamics of AdS space-times

Daniel Santos-Oliván

Institut de Ciències de l'Espai (CSIC-IEEC), Campus UAB, 08193 Bellaterra, Spain

E-mail: santos@ice.cat

Carlos F. Sopuerta

Institut de Ciències de l'Espai (CSIC-IEEC), Campus UAB, 08193 Bellaterra, Spain

E-mail: sopuerta@ieec.uab.es

Abstract. In the last years, the stability of Anti-de Sitter (AdS) space-times has attracted a lot of attention. Not only because of its own importance but primarily due to the AdS/CFT correspondence that conjectures an equivalence between a string theory on an asymptotically AdS space-time and a conformally invariant quantum field theory (CFT). Recently, Bizon and Rostworowski (2011) showed that the boundary of AdS prevents energy from dispersing. As a consequence, AdS perturbations will collapse after bouncing back from the AdS boundary a sufficient number of times for their energy to be concentrated enough. The details of the mechanisms that triggers the instability are currently an active topic of discussion. Here, we present a new approach to the problem of the collapse of a massless scalar field that introduces a transition from a Cauchy-based evolution to a characteristic one that is able to track with greater accuracy the latest stages of the collapse.

1. Introduction

The interest in the study of space-times with negative cosmological constant is very recent. Although AdS is a maximally symmetric solution to Einstein's field equations known since a long time ago, physicists have ignored this space-time and even classical books of General Relativity rarely mention it (one notable exception is the Hawking and Ellis book [1]). The establishment of the gauge/gravity duality through the AdS/CFT correspondence shown by Maldacena [2] have changed the scenario completely, generating a lot of activity. As in the case of Minkowski and de Sitter space-times, AdS space-time has been shown to be stable under linear (infinitesimal) perturbations [3], but the problem of non-linear perturbations of AdS is still under debate. Different numerical simulations have shown, in contrast to the Minkowski and de Sitter cases, instabilities in the dynamics of real [4, 5] and complex [6] massless scalar fields in AdS space-times. However, some works indicate there may exist states free from instabilities [7, 8]. There have also been attempts to study the AdS stability with purely analytic means [9, 10, 11, 12]. In addition, there are some studies on the role of the AdS boundary that consider space-times without cosmological constant but with reflecting boundaries [13, 14, 15].

We address the problem of the collapse of a massless scalar field in an Asymptotically AdS (AAdS) space-times from a new point of view. We start with a Cauchy evolution scheme in order to follow the evolution through the different bounces at the AdS boundary, but then we



introduce a transition to a characteristic evolution scheme to follow the last stages of the collapse with much more resolution (more details will appear in [16]).

2. Dynamics of AAdS space-times

The dynamics of a self-gravitating real massless scalar field ϕ in an AAdS space-time of dimension $d + 1$ is described by the Einstein-Klein-Gordon field equations:

$$G_{\mu\nu} + \Lambda g_{\mu\nu} = (d-1) \left(\nabla_\mu \phi \nabla_\nu \phi - \frac{1}{2} g_{\mu\nu} \nabla_\alpha \phi \nabla^\alpha \phi \right), \quad g^{\mu\nu} \nabla_\mu \nabla_\nu \phi = 0, \quad (1)$$

where $g_{\mu\nu}$ ($\mu, \nu = 0, \dots, d$) is the space-time metric (and ∇_μ the associated canonical covariant derivative), $\Lambda < 0$ is the cosmological constant, and $G_{\mu\nu}$ is the Einstein tensor.

We solve these equations by using a Cauchy-characteristic scheme. We start with Cauchy evolution using a system of coordinates where the AdS boundary (reachable in a finite time by the scalar field propagation) is at a finite coordinate distance. In this way we can follow the evolution of the scalar field, which typically will bounce at the AdS boundary a finite number of times before collapsing [4, 6]. When the collapse is approaching we need a high resolution to control the gradients in the field that signal the formation of an apparent horizon (AH). We have noticed that a multidomain pseudospectral method with adaptive refinement of the domains is still not enough for many purposes, although it provides a high accuracy for most parts of the evolution. To deal with this we have designed a numerical scheme that makes a transition from the Cauchy evolution to a characteristic one where each point follows an ingoing null geodesic. This allows us to follow much better the collapse.

2.1. Cauchy evolution

The metric of a $d+1$ -dimensional spherically symmetric AAdS space-time can be written as [4, 5]

$$ds^2 = \frac{\ell^2}{\cos^2(x)} \left(-A(t, x) e^{-2\delta(t, x)} dt^2 + \frac{dx^2}{A(t, x)} + \sin^2(x) d\Omega_{d-1}^2 \right), \quad (2)$$

where ℓ is the AdS length scale, defined as $\ell^2 = -d(d-1)/2\Lambda$, and $d\Omega_{d-1}^2$ is the line element of a $d-1$ -sphere. The important point is that x is a radial compactified coordinate with range $[0, \pi/2]$, being $x = 0$ the origin and $x = \pi/2$ the AdS boundary. We recover pure AdS by taking $A = 1$ and $\delta = 0$. Our evolution equations for (A, δ, ϕ) are a modification of the ones in [4, 5].

2.2. Characteristic evolution

We have adapted the scheme first introduced by Christodoulou [17] and later used by [18, 19] for AAdS space-times. The starting point is the spherically-symmetric metric

$$ds^2 = -g\bar{g} du^2 - 2g du dr + r^2 d\Omega_{d-1}^2, \quad (3)$$

where u is an ingoing null coordinate and r is a radial one (the AdS boundary is at $r \rightarrow \infty$). The functions $g = g(u, r)$ and $\bar{g} = \bar{g}(u, r)$ are always greater than some normalization value at the origin that we choose to be 1. Pure AdS is recovered by taking $g = 1$ and $\bar{g} = 1 + r^2/l^2$. The scalar field is described by the following two variables:

$$\bar{h} \equiv \phi, \quad h \equiv \phi + \frac{2r}{d-1} \phi_{,r} \quad \Rightarrow \quad \bar{h}(u, r) = \frac{1}{r} \int_0^r dr' h(u, r'). \quad (4)$$

The metric functions can be recovered from the scalar field variables from the expressions:

$$g(u, r) = \exp \left\{ \frac{(d-1)^2}{4} \int_0^r dr' \frac{(h(u, r') - \bar{h}(u, r'))^2}{r'} \right\}, \quad (5)$$

$$\bar{g}(u, r) = \frac{1}{r^{d-2}} \int_0^r dr' \left(d - 2 + d \frac{r'^2}{\ell^2} \right) r'^{d-3} g(u, r'). \quad (6)$$

The characteristic evolution consists in evolving the variables along ingoing geodesics from one $u = \text{const.}$ null slide to the next one. In this way the radial coordinate of a grid point obeys the following evolution equation [see Eq. (3)]:

$$\frac{dr}{du} = -\frac{1}{2}\bar{g}. \quad (7)$$

The idea is to evolve the scalar field variable h from one null slice $u = \text{const.}$ to the next one along the ingoing null geodesics of Eq. (7), while the rest of variables (\bar{h}, \bar{g}, g) can be obtained from h by radial integration according to Eqs. (4), (5), and (6). The equation for h comes from the Klein-Gordon equation and using that along the ingoing null geodesics we have

$$\frac{dh(u, r(u))}{du} = \left(\frac{\partial h}{\partial u} \right)_{r=r(u)} + \left(\frac{\partial h}{\partial x} \right)_{r=r(u)} \frac{dr(u)}{du}, \quad (8)$$

where $r(u)$ is a solution of Eq. (7). Then

$$\frac{dh}{du} = \frac{d-2}{2r} (h - \bar{h}) \left[\left(1 + \frac{d}{d-2} \frac{r^2}{\ell^2} \right) g - \frac{d-1}{2(d-2)} \bar{g} \right]. \quad (9)$$

2.3. Transition from Cauchy to characteristic evolution

In order to use the characteristic evolution to follow the collapse, we need to construct initial data at an initial null slide $u = u_o = \text{const.}$ from the results of the Cauchy evolution. To that end we have to translate the information from a set of $t = \text{const.}$ slides coming from the Cauchy evolution to the values of the variable h , the one we evolve from one null slide to the next one, at the initial null slide $u = u_o$. A key ingredient to perform this transformation is the following relations between Cauchy and characteristics variables:

$$h = \phi + \sin(x) \cos(x) \frac{U_- + U_+}{2}, \quad U_{\pm} = \partial_x \phi \pm \frac{e^{\delta}}{A} \partial_t \phi, \quad (10)$$

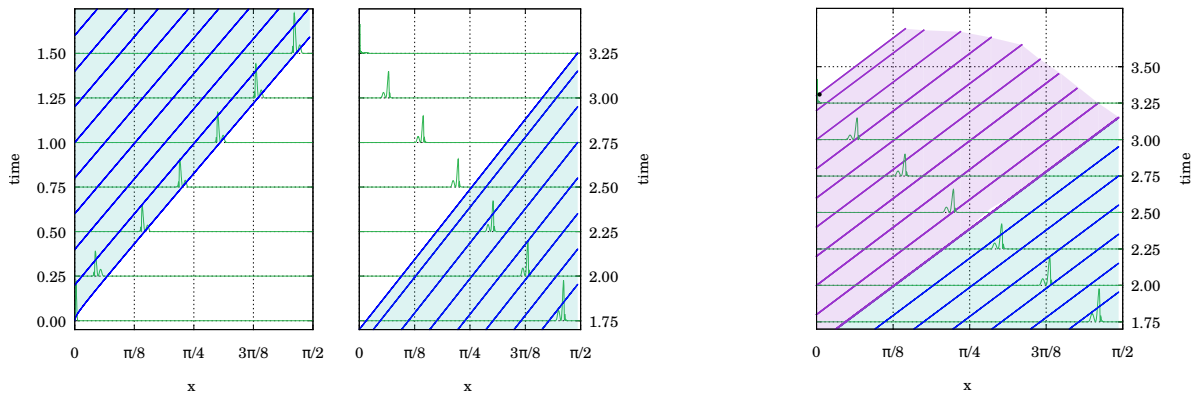


Figure 1. Green lines show data obtained from the Cauchy evolution and blue ones the outgoing null geodesics constructed to initialize the characteristic evolution. In the left figures the data generated by a complete Cauchy evolution is shown and, in the right one, the purple area indicates data obtained from the characteristic evolution.

where U_{\pm} are characteristic fields of the Klein-Gordon equation (with propagation speeds $\pm Ae^{-\delta}$) so that the set of variables (ϕ, U_{\pm}) leads to a first-order hyperbolic system for the Cauchy evolution. Another key ingredient is the relation between the coordinate systems used for the Cauchy and characteristic evolutions. The relation between radial coordinates is quite simple: From Eqs. (2) and (3) it is just $r = \ell \tan(x)$. We do not have an expression for the null coordinate u in terms of (t, x) , instead the $u = \text{const.}$ null slices have to be obtained from the equations for the outgoing null geodesics in (t, x) coordinates:

$$\frac{dx}{dt} = +Ae^{-\delta}, \quad (11)$$

which can be integrated from the origin using the Cauchy evolution data. From the coordinate change we can derive the relation

$$A = \frac{\bar{g}}{g \left(1 + \frac{r^2}{\ell^2}\right)}, \quad (12)$$

which can be used to track the formation of an AH in the characteristic evolution ($A \rightarrow 0$). The Cauchy-characteristic transition is illustrated in figure 1. In the left plot, the green lines (horizontal) represent the data generated by the Cauchy evolution. In each frame, we can start an outgoing null geodesic ($u = \text{const.}$) from $x = 0$ using Eq. (11) and compute where this geodesic will be in the next step and store the data for both x (or r) and the field h . We can construct in this way several null outgoing geodesics and then perform the Cauchy-characteristic transition using the one that has the optimal initial conditions.

3. Comparing the Cauchy and characteristic evolution schemes

In this section, for the case of $d = 3$, we compare a simulation done only with Cauchy evolution with another one that starts with Cauchy evolution but changes to characteristic evolution near the collapse. In the first case, as we approach the collapse, the scalar field develops a steep profile. Then, in order to maintain the accuracy and stability of the code we have to introduce more resolution, making the simulation much slower. In the other case, we can change before the profile becomes steep making the Cauchy evolution stage much faster. In the characteristic evolution stage we do not need to introduce more points because the null slicing adapts to the

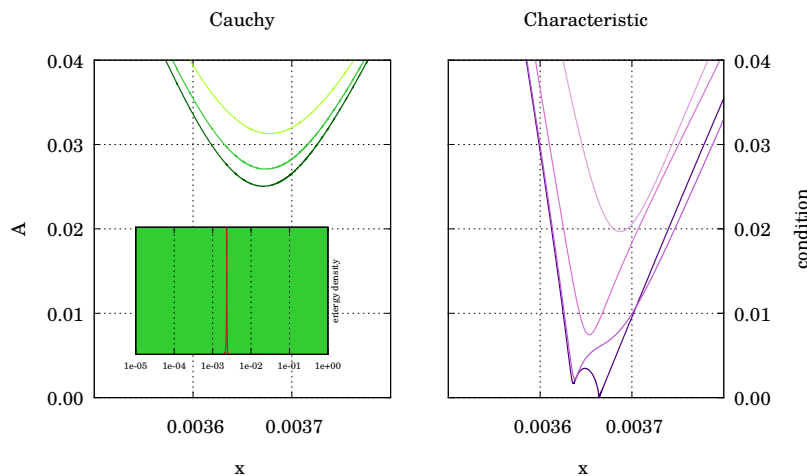


Figure 2. Comparison between the Cauchy and characteristic evolutions. AH formation occurs when $A \rightarrow 0$.

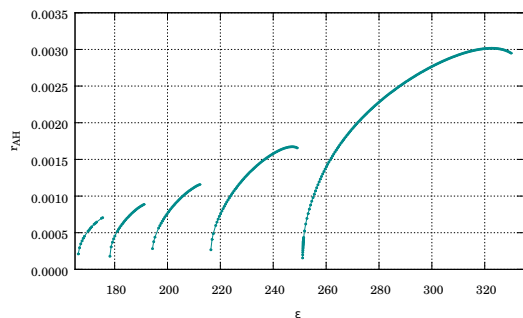


Figure 3. AH radius (r_{AH}) with respect to amplitude (ϵ). The number of bounces at the AdS boundary changes from branch to branch (see text for details).

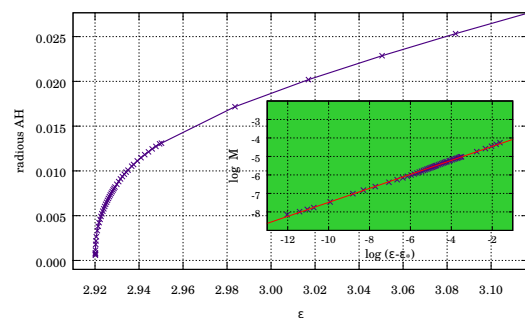


Figure 4. Critical exponent obtained using characteristic initial data and purely characteristic evolution. The value obtained is $\gamma \sim 0.378$.

horizon formation concentrating a large portion of the points in the region we are interested in. This is illustrated in figure 2, where the small plot in the left shows the steep profile generated in the energy density (notice the logarithmic scale in x). The plots shows A for both evolutions (in the characteristic case it is estimated using Eq. (12)). The computational time used for the two plots is similar. It is clear that the characteristic evolution adapts much better to our problem, allowing us to go much closer to the AH formation ($A \rightarrow 0$). The right plot shows how important is to get as close as possible to AH formation since at some point the profile of A generates structure at *small* scales.

4. Results and discussion

Using the method of the Cauchy-characteristic transition presented above, we can define our initial conditions as:

$$U_-(t=0, x) = +\epsilon \cos^{d-2}(x) e^{\frac{4 \tan^2(x)}{\pi^2 \omega^2}}, \quad U_+(t=0, x) = -\epsilon \cos^{d-2}(x) e^{\frac{4 \tan^2(x)}{\pi^2 \omega^2}}, \quad (13)$$

where ϵ and ω , the amplitude and width of the initial profile respectively, are free parameters. We have adopted a fixed value for ω ($\omega = 0.05$) and have performed evolutions for a large number of values for the amplitude ϵ . For sufficient large amplitudes the field collapses in way very similar to what Choptuik described in the asymptotically-flat case [20]. This is problematic in our scheme because the time of collapse for this kind of simulations is smaller than the time that we typically need to construct an initial geodesic to initialize the characteristic evolution. For relatively small amplitudes, the field tries to collapse but fails and then it disperses. In the asymptotically-flat case the field will completely disperse and the end state of the evolution is Minkowski space-time. In the case of AAdS spacetimes the field eventually (in a finite time) bounces at the AdS boundary and comes back towards the origin where it will collapse provided certain conditions are satisfied, otherwise the field will disperse again and bounce at the AdS boundary. This will happen a number of times until the field will finally collapse. In figure 3 we can see some results from numerical simulation for initial configuration with amplitudes in the range $\epsilon \in [160, 330]$. The right branch correspond to initial conditions that collapse after just one bounce at the AdS boundary. Each branch to the left corresponds to configurations that go through one additional bounce (the left branch corresponds to configurations that went through five bounces). This behavior was reported in [4] and the evidence indicates that after each bounce the energy is transferred from lower to higher frequency modes [21, 22].

Up to now we have discussed simulations that use the Cauchy-characteristic transition. Another possibility is to use only the characteristic evolution, by prescribing initial configurations

at a $u = u_o = \text{const.}$ null surface (an outgoing null geodesic) and by evolving it using our characteristic code. Since these simulations do not cover the whole space-time (see figure 1) we can only use them for configurations are always within the space-time region covered by the characteristic evolution. An example of this are configurations that collapse directly without bounces at the AdS boundary. For those we use initial conditions given by

$$\phi = \bar{h}(u = 0, r) = \epsilon r^2 e^{-\frac{(r-r_0)^2}{\omega^2}}. \quad (14)$$

Fixing $\omega = 0.05$ and $r_0 = 0.1$, we can vary the amplitude ϵ and only consider those configurations that form an AH. The others, which disperse, correspond to evolutions with bounces, but we cannot track them with the characteristic evolution. Around $\epsilon = \epsilon_* \sim 2.92$, we observe critical behavior: The black hole mass at the AH formation scales as: $M_{AH} \sim (\epsilon - \epsilon_*)^\gamma$, where $M_{AH} = r_{AH} (1 + (r_{AH}/\ell)^2) / 2$. The analysis of this case can be seen in figure 4. By fitting our results in the region close to the critical amplitude, $\epsilon_* = 2.920151$, we obtain a critical exponent of $\gamma \sim 0.378$. This result is compatible with the one obtained first by Choptuik [20]. This is something that was anticipated by Bizon and Rostworowski [4] and that here we confirm with one more digit of precision.

To sum up, we have introduced a new scheme for the study of the dynamics of spherically symmetric AAdS space-times, in particular the fate of instabilities, which is based on a combined Cauchy-characteristic evolution that provides higher precision to follow collapse and the formation of an AH. We have also presented results from simulations that confirm recent findings in the literature obtained with other evolution schemes.

Acknowledgments

We acknowledge support from contracts 2009-SGR-935 (AGAUR), AYA-2010-15709 (MICINN), ESP2013-47637-P (MINECO) and the computational resources provided by CESGA (CESGA-ICTS-266). DSO acknowledges the FPI PhD contract BES-2012-057909.

References

- [1] Hawking S W and Ellis G F R 1973 *The large scale structure of space-time* (Cambridge: Cambridge University Press)
- [2] Maldacena J M 1999 *Int.J.Theor.Phys.* **38** 1113–1133 (*Preprint hep-th/9711200*)
- [3] Ishibashi A and Wald R M 2004 *Class.Quant.Grav.* **21** 2981–3014 (*Preprint hep-th/0402184*)
- [4] Bizon P and Rostworowski A 2011 *Phys.Rev.Lett.* **107** 031102 (*Preprint 1104.3702*)
- [5] Jalmuzna J, Rostworowski A and Bizon P 2011 *Phys.Rev.* **D84** 085021 (*Preprint 1108.4539*)
- [6] Buchel A, Lehner L and Liebling S L 2012 *Phys.Rev.* **D86** 123011 (*Preprint 1210.0890*)
- [7] Buchel A, Liebling S L and Lehner L 2013 *Phys.Rev.* **D87** 123006 (*Preprint 1304.4166*)
- [8] Maliborski M and Rostworowski A 2013 *arXiv* (*Preprint 1307.2875*)
- [9] Holzegel G and Smulevici J 2012 *Annales Henri Poincaré* **13** 991–1038 (*Preprint 1103.0712*)
- [10] Ishibashi A and Maeda K 2012 *Phys.Rev.* **D86** 104012 (*Preprint 1208.1563*)
- [11] Holzegel G H and Warnick C M 2013 (*Preprint 1312.5332*)
- [12] Friedrich H 2014 *Class.Quant.Grav.* **31** 105001 (*Preprint 1401.7172*)
- [13] Maliborski M 2012 *Phys.Rev.Lett.* **109** 221101 (*Preprint 1208.2934*)
- [14] Okawa H, Cardoso V and Pani P 2014 *Phys.Rev.* **D89** 041502 (*Preprint 1311.1235*)
- [15] Okawa H, Cardoso V and Pani P 2014 *Phys.Rev.* **D90** 104032 (*Preprint 1409.0533*)
- [16] Santos-Oliván D and Sopuerta C F A new scheme for the numerical evolution of AAdS space-times In preparation
- [17] Christodoulou D 1986 *Commun.Math.Phys.* **105** 337–361
- [18] Goldwirth D S and Piran T 1987 *Phys.Rev.* **D36** 3575
- [19] Garfinkle D 1995 *Phys.Rev.* **D51** 5558–5561 (*Preprint gr-qc/9412008*)
- [20] Choptuik M W 1993 *Phys.Rev.Lett.* **70** 9–12
- [21] Bizoń P and Jalmuna J 2013 *Phys.Rev.Lett.* **111** 041102 (*Preprint 1306.0317*)
- [22] Maliborski M and Rostworowski A 2014 *Phys.Rev.* **D89** 124006 (*Preprint 1403.5434*)